Coupled Plasmonic Nanoantennas

Hancong Wang[1,2,3(✉)]

[1] Fujian Provincial Key Laboratory for Automotive Electronics and Electric Drive, Fuzhou 350108, China
whcuser@163.com
[2] Fujian Provincial Key Laboratory of Digital Equipment, Fuzhou 350108, China
[3] School of Information Science and Engineering, Fujian University of Technology, Fuzhou 350108, China

Abstract. The electromagnetic coupling between metal nanoparticles lead to a variety of fundamental studies and practical applications in plasmonics. For example, by strong coupling between metallic nanostructures, plasmonic antennas are able to concentrate and re-emit light in a controllable way. A variety of structures of optical antennas have been investigated in the past decade. In this review, we will discuss the coupled plasmonic nanoantennas from the typical applications point of view, i.e., control of local intensity, control of emission direction, control of far-field polarization, and outlook the corresponding impacts in understanding physics.

Keywords: Plasmonics · Nanoantennas · Coupling · Generalized Mie theory

1 Introduction

Antennas appeared a century ago was first used to transmit and collect radio and microwave which now play an essential role in the modern wireless world [1–4]. Optical antennas as an analogue at the nanoscale are of great interest due to the unique ability of controlling absorption and emission at visible and infrared region [4, 5], such as focusing optical fields to sub-diffraction limited volumes [6–8], enhance the excitation and emission of molecules [9, 10] and quantum emitters [11, 12] and modify their spectrum and lifetime [13, 14]. Propagating light can be converted into nanoscale enhanced near field [15–18], and vice versa, a localized excitation can be coupled to directed radiation. The efficiency of an optical antenna depends on its shape, material, dimension, geometry, and operation frequency [19, 20]. Various optical antennas have been developed experimentally and theoretically, such as individual discs [21], triangles [22, 23], flowers [24], as well as coupled antenna such as dimers [3, 25], bowties [8, 13], trimers [10], etc. [26–28]. Most of these antennas are based on metallic nanostructures that support surface plasmons (SP) [29, 30], so called plasmonic antennas. Single and coupled nanoantennas have been investigated thoroughly by far-field spectroscopy, exploiting two-photon luminescence [9, 31] and near-field scanning microscope [4, 22, 32]. Abundant applications have been found in surface enhanced Raman scattering [6, 33], optical manipulation [25, 34], biosensing [35, 36] and integrated photonic devices [37–39], etc.

J. Pan et al. (eds.), *Intelligent Data Analysis and Applications*, Advances in Intelligent Systems and Computing 535, DOI 10.1007/978-3-319-48499-0_31

Here we provide an overview of the coupled antenna system, e.g. coupled nanorod, bow-tie and nano-aggregates, etc. Light properties such as the intensity, polarization and direction of emission, can be controlled effectively by different geometries of nanoantennas, and will be discussed respectively.

2 Control of Local Intensity

To enhance the performance of nanoantennas, the way of plasmonic coupling between nanostructures are usually adopted. Figure 1a shows two nanorod with the length 500 nm separated about 40 nm [9]. The coupling between these two rods gives rise to strong local enhancement which is detected by the intensity of TPL. More experiments and theoretical calculations indicate that, the intensity enhancement at the visible frequencies can be as high as 10^3 when the gap reduced to a few of nanometers.

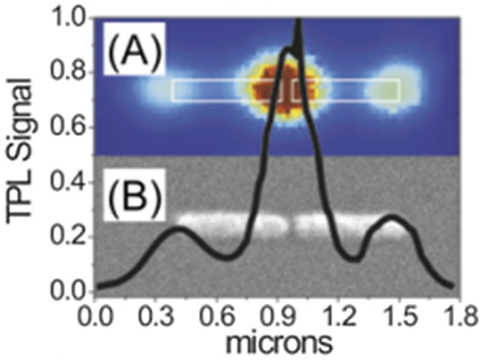

Fig. 1. (Reproduced from [9]) (a) TPL scans for two 500 nm long gold bar with a 40 nm gap and (b) the SEM image: The superimposed black lines plot the TPL signal along the symmetry axis of the antennas.

The bow-tie structures [13] are one of the most investigated configurations. The enhancement factor of $|E|^2/|E_0|^2$ at the gap of the bow-tie antenna is evaluated by the surface-enhanced fluorescence which is shown in Fig. 2. The size of the gap varies from 15 nm to 80 nm. The maximum enhancement of fluorescence f_F can reach to 1340-fold.

More systematic study was done by Schnell et al., where they investigated the near-field oscillations of progressively loaded plasmonic antennas at infrared frequency by scattering-type scanning near-field optical microscopy [4]. In Fig. 3a the amplitude signals at the both ends of the nanorod and phase change at the rod center, clearly reveals the dipolar mode excited at a continuous nanorod. When a wedge is cut at the middle, the dipolar mode of the nanorod still holds which is shown in Fig. 3b. But, if the rod is cut more deeply and even fully cut, the case is completely different. In Fig. 3c, the bridge between the two rods is only 2 % of the cross-section, which cannot restore the dipolar mode any more. For the fully cut rod in Fig. 3d, a gap (80 nm) is formed in the rod center. Each antenna segment oscillates as a dipole. Hence, a face change exists between the two segments and the gap.

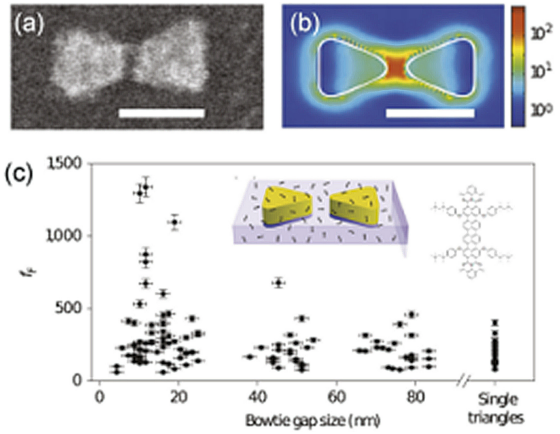

Fig. 2. (Reproduced from [13]) (a) SEM image of a gold bowtie antenna. Scale bar = 100 nm. (b) Calculation of the local electric field intensity enhancement. (c) Enhancement factor, f_F, from several nanoantennas as function of the gap size. Inset: Schematic representation of molecules randomly placed around a gold bowtie antenna on a transparent substrate.

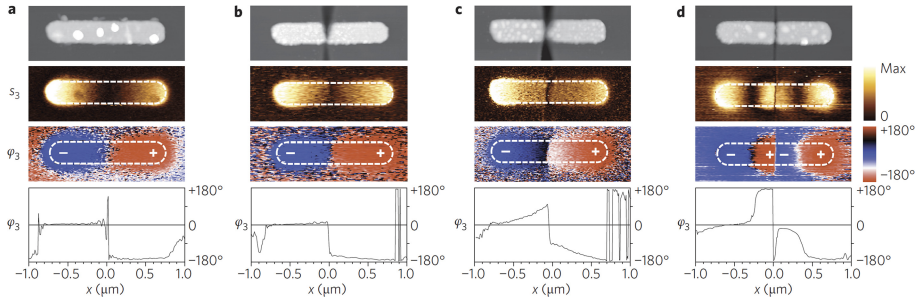

Fig. 3. (Reproduced from [4]) Near-field images of progressively loaded nanoantennas at a wavelength of 9.6 m. (a) Continuous rod antenna. (b) Low-impedance loaded antenna where a thick metal bridge connects the two antenna segments. (c) High-impedance loaded antenna where a tiny metal bridge connects the two antenna segments. (d) Fully cut antenna where the two antenna segments are completely separated. Experimental results showing topography and near-field amplitude and phase images.

3 Control of Emission Direction

Controlling the far-field emission from an emitter is another important property of nanoantennas. For an emitter such as quantum dot, the emission direction involves a large solid angle. To beaming the emission, a Yagi-Uda plasmonic antenna are developed [11]. In Fig. 4, a quantum dot is positioned near one of the arm of the antenna. The constructive interference of the emission from each arm excited by the emitter results in a narrow directional radiation pattern. The gap between each arm in Yagi-Uda is about 100 nm, which is relative large for plasmonic coupling.

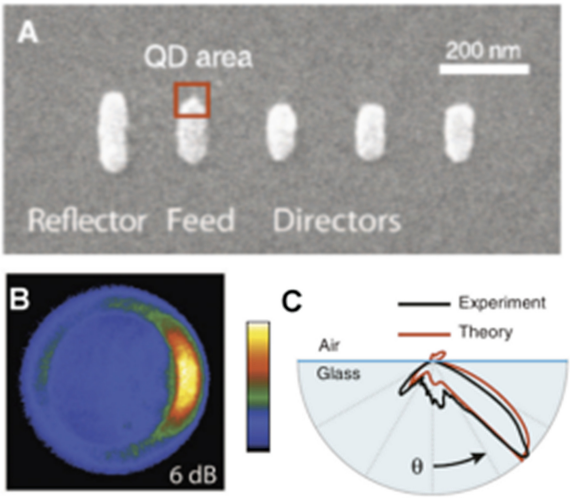

Fig. 4. (Reproduced from [11]) (a) SEM image of a five-element Yugi-Uda gold nanoantenna. A quantum dot is attached to one end of an arm, indicated with a red square. (b) Radiation pattern (intensity distribution at the back focal plane of the objective) from Yagi-Uda after an 830-nm long-pass filter. (c) Measurement (black line) and calculation (red line) of the radiation angular distribution for the structure. (Color figure online)

A stronger coupling case is shown in Fig. 5 [40]. The scattering properties can be tuned by two closely spaced silver and gold disks. Interestingly, the direction of the scattering is dependent on the wavelength. For blue light at 450 nm and red light at 700 nm, the scattering is in opposite directions shown in Fig. 5b, which can be used as an ultra-small $\sim\lambda/100$ photon-sorting nanodevice.

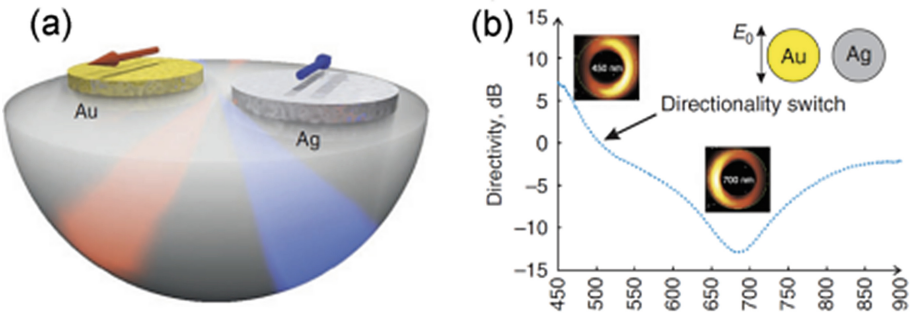

Fig. 5. (Reproduced from [40]) (a) An artist's view of colour routing from a bimetallic dimer supported by a glass substrate. (b) Experimental directivities as a function of wavelength. Insets: corresponding direct and Fourier color images. Radiation patterns recorded at specific wavelengths corresponding to scattering to the right (450 nm) and to the left (700 nm). (Color figure online)

4 Control of Far-Field Polarization

Not only the intensity and direction, but also light polarization from an emitter such as Raman scattering (RS) of molecules in the gap between nanoantennas can be manipulated significantly [10, 41]. First a simplest case of a nanocrystal dimer is considered. Figure 6a shows the SEM image of such a dimer, and it is seen that the angle of the dimer axis, is $\sim 130°$ with respect to the x axis. This angle is corresponding to the maximal RS intensity shown in the Fig. 6b by black and red dots, which means the favorite incident polarization of the laser for the enhancement is along the dimer axis for both Raman shift (773 cm^{-1} and 1650 cm^{-1}). Here the low concentration of molecules used ensures that each aggregate contains no more than a single molecule [42]. The depolarization ρ in Fig. 6c is defined as $\rho = (I_{//} + I_{\perp})/(I_{//} + I_{\perp})$, where $I_{//}$and $I_{\perp}$ are RS signals with orthogonal polarization, which indicates the polarization of the RS light is also along the dimer axis at these two frequencies. These properties of dimer can be simulated by treating the nanoparticles as spheres. As the single molecule Raman signal can only from "hot sites", the calculations are concentrated on the field enhancement in the junction of the dimer at the laser wavelength, and the depolarization of the emission from a dipole situated in this junction. The calculated results shown by the curves in Fig. 6b and c are consistent to the experiment. This expected agreement is actually due to the axial symmetric geometry of the dimer.

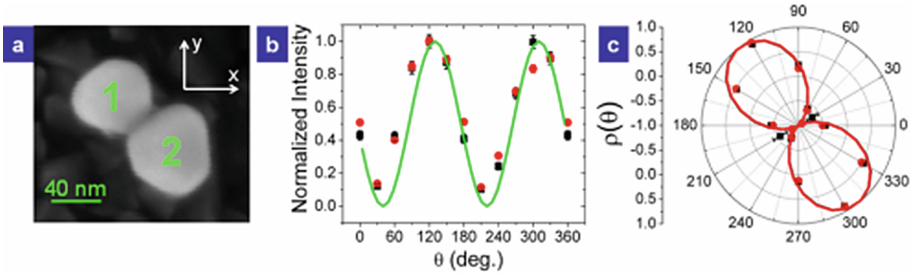

Fig. 6. (Reproduced from [10]) Polarization response of a nanocrystal dimer. (a) A SEM image shows a dimer of nanoparticles, which is tilted ~ 1300 from the x direction. (b) Normalized SERS intensity at 555 nm (black squares) and 583 nm (red circles) as a function of the angle of rotation by the λ/2 waveplate. The green line is the result of the generalized Mie theory calculation of the normalized local field enhancement factor at λ = 532 nm, using the geometry from the SEM image as the only input. (c) Depolarization ratio (ρ) measured at 555 nm (back squares) and 583 nm (red circles). Black and red lines show the result of Mie theory calculation performed at 555 nm and 583 nm, respectively. (Color figure online)

A drastically different behavior is obtained from the trimer shown in Fig. 7. The intensity profile in Fig. 7b is maximal at an angle of $\sim 75^{\circ}$, which is close to the axis of 1st and 2nd nanoparticles. Whereas, the depolarization ratio profiles do not coincide with each other and in addition they are both rotated with respect to the intensity profile. The depolarization pattern of the 555 nm light is rotated by $\sim 45^{\circ}$, while the 583 nm light is rotated by $\sim 75^{\circ}$. In order to simulate this situation of trimer, calculation was performed

by assuming that the molecule is placed in turn in each of the three possible junctions. Only when the molecule is set in the junction marked with a red arrow in Fig. 7a, the calculated and experimental results are in good agreement for both normalized intensity and depolarization, which also confirms the assumption that only one molecule in the junction, contributes to the signal. What should be note is this counter-intuitive wavelength-dependent polarization rotation is not an accident. The rotation only exists in the cases with the number of the particles are larger than two.

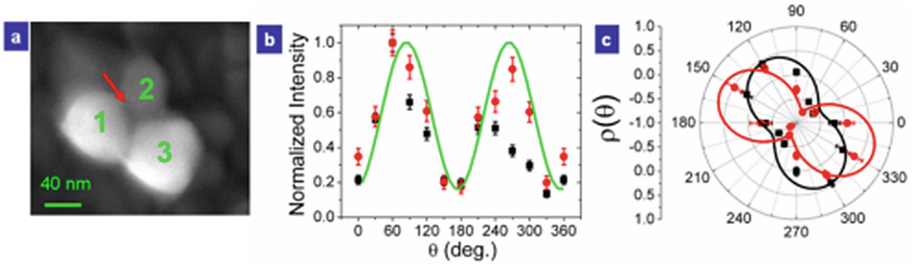

Fig. 7. (Reproduced from [10]) Polarization response of a nanocrystal trimer. (a) SEM image of the trimer. (b) Normalized SERS intensity at 555 nm (black squares) and 583 nm (red circles) as a function of the angle of rotation by the λ/2 waveplate. The intensities at both wavelengths show approximately the same profile, but the maximal intensity is observed at ∼75°, which does not match any pair of nanoparticles in the trimer. The green line the result of a calculation assuming that the molecule is situated at the junction marked with red arrow in SEM image. (c) Depolarization ratio (ρ) measured at 555 nm (back squares) and 583 nm (red circles). The black and red lines show the result of calculations at the two wavelength, assuming that the molecule is situated at the junction marked with red arrow in SEM image. (Color figure online)

5 Summary

Various coupled nanoantennas have been introduced here. Plasmonic antennas can be used to manipulate light properties at the nanoscale. Compare with single structures, more important nanoantennas are coupled systems, such as nanorod with small gap, bow-tie, Yugi-Uda structure and nanoparticle aggregates, etc. With the help of SP coupling, light intensity, direction and polarization can be well tailed. Although there are still a lot of unsolved problems, it is no doubt, nanoantennas as a new subject will be further developed, and more applications will be found in, such as ultra-sensitive sensor, and biosensing, integrated photonic devices, etc.

Acknowledgements. This work was supported by the Startup Foundation of Fujian University of Technology (GY-Z160049), the Mid-youth Project of Education Bureau of Fujian Province (JAT160331), and the Fujian Provincial Major Research and Development Platform for the Technology of Numerical Control Equipment (2014H2002).

References

1. Greffet, J.J.: Nanoantennas for light emission. Science **308**, 1561–1563 (2005)
2. Mühlschlegel, P., Eisler, H.J., Martin, O.J.F., Hecht, B., Pohl, D.W.: Resonant optical antennas. Science **308**, 1607–1609 (2005)
3. Shegai, T., Miljkovic, V.D., Bao, K., Xu, H.X., Nordlander, P., Johansson, P., Kall, M.: Unidirectional broadband light emission from supported plasmonic nanowires. Nano Lett. **11**, 706–711 (2011)
4. Schnell, M., Garcia-Etxarri, A., Huber, A.J., Crozier, K., Aizpurua, J., Hillenbrand, R.: Controlling the near-field oscillations of loaded plasmonic nanoantennas. Nat. Photonics **3**, 287–291 (2009)
5. Giannini, V., Fernandez-Dominguez, A.I., Heck, S.C., Maier, S.A.: Plasmonic nanoantennas: fundamentals and their use in controlling the radiative properties of nanoemitters. Chem. Rev. **111**, 3888–3912 (2011)
6. Xu, H.X., Bjerneld, E.J., Käll, M., Börjesson, L.: Spectroscopy of single hemoglobin molecules by surface enhanced ranman scattering. Phys. Rev. Lett. **83**, 4357–4360 (1999)
7. Zhang, Z., Weber-Bargioni, A., Wu, S.W., Dhuey, S., Cabrini, S., Schuck, P.J.: Manipulating nanoscale light fields with the asymmetric bowtie nano-colorsorter. Nano Lett. **9**, 4505–4509 (2009)
8. Fromm, D.P., Sundaramurthy, A., Schuck, P.J., Kino, G., Moerner, W.E.: Gap-dependent optical coupling of single "Bowtie" nanoantennas resonant in the visible. Nano Lett. **4**, 957–961 (2004)
9. Ghenuche, P., Cherukulappurath, S., Taminiau, T.H., van Hulst, N.F., Quidant, R.: Spectroscopic mode mapping of resonant plasmon nanoantennas. Phys. Rev. Lett. **101**, 116805 (2008)
10. Shegai, T., Li, Z.P., Dadosh, T., Zhang, Z., Xu, H.X., Haran, G.: Managing light polarization via plasmon–molecule interactions within an asymmetric metal nanoparticle trimer. Proc. Nat. Acad. Sci. U.S.A. **105**, 16448–16453 (2008)
11. Curto, A.G., Volpe, G., Taminiau, T.H., Kreuzer, M.P., Quidant, R., van Hulst, N.F.: Unidirectional emission of a quantum dot coupled to a nanoantenna. Science **329**, 930–933 (2010)
12. Ringler, M., Schwemer, A., Wunderlich, M., Nichtl, A., Kurzinger, K., Klar, T.A., Feldmann, J.: Shaping emission spectra of fluorescent molecules with single plasmonic nanoresonators. Phys. Rev. Lett. **100**, 203002 (2008)
13. Kinkhabwala, A., Yu, Z.F., Fan, S.H., Avlasevich, Y., Mullen, K., Moerner, W.E.: Large single-molecule fluorescence enhancements produced by a bowtie nanoantenna. Nat. Photonics **3**, 654–657 (2009)
14. Farahani, J.N., Pohl, D.W., Eisler, H.J., Hecht, B.: Single quantum dot coupled to a scanning optical antenna: a tunable superemitter. Phys. Rev. Lett. **95**, 017402 (2005)
15. Knight, M.W., Grady, N.K., Bardhan, R., Hao, F., Nordlander, P., Halas, N.J.: Nanoparticle-mediated coupling of light into a nanowire. Nano Lett. **7**, 2346–2350 (2007)
16. Li, Z.P., Hao, F., Huang, Y.Z., Fang, Y.R., Nordlander, P., Xu, H.X.: Directional light emission from propagating surface plasmons of silver nanowires. Nano Lett. **9**, 4383–4386 (2009)
17. Li, Z.P., Zhang, S.P., Halas, N.J., Nordlander, P., Xu, H.X.: Coherent modulation of propagating plasmons in silver-nanowire-based structures. Small (Weinheim an der Bergstrasse, Germany) **7**, 593–596 (2011)

18. Li, Z.P., Bao, K., Fang, Y.R., Guan, Z.Q., Halas, N.J., Nordlander, P., Xu, H.X.: Effect of a proximal substrate on plasmon propagation in silver nanowires. Phys. Rev. B **82**, 241402 (2010)
19. Wiley, B.J., Chen, Y.C., McLellan, J.M., Xiong, Y.J., Li, Z.Y., Ginger, D., Xia, Y.N.: Synthesis and optical properties of silver nanobars and nanorice. Nano Lett. **7**, 1032–1036 (2007)
20. Liang, H.Y., Yang, H.X., Wang, W.Z., Li, J.Q., Xu, H.X.: High-yield uniform synthesis and microstructure-determination of rice-shaped silver nanocrystals. J. Am. Chem. Soc. **131**, 6068–6069 (2009)
21. Langhammer, C., Kasemo, B., Zoric, I.: Absorption and scattering of light by Pt, Pd, Ag, and Au nanodisks: absolute cross sections and branching ratios. J. Chem. Phys. **126**, 194702–194711 (2007)
22. Rang, M., Jones, A.C., Zhou, F., Li, Z.Y., Wiley, B.J., Xia, Y.N., Raschke, M.B.: Optical near-field mapping of plasmonic nanoprisms. Nano Lett. **8**, 3357–3363 (2008)
23. Nelayah, J., Kociak, M., Stephan, O., de Abajo, F.J.G., Tence, M., Henrard, L., Taverna, D., Pastoriza-Santos, I., Liz-Marzan, L.M., Colliex, C.: Mapping surface plasmons on a single metallic nanoparticle. Nat. Phys. **3**, 348–353 (2007)
24. Liang, H.Y., Li, Z.P., Wang, W.Z., Wu, Y.S., Xu, H.X.: Highly surface-roughened "Flower-like" silver nanoparticles for extremely sensitive substrates of surface-enhanced raman scattering. Adv. Mater. **21**, 4614–4618 (2009)
25. Svedberg, F., Li, Z.P., Xu, H.X., käll, M.: Creating hot nanoparticle pairs for surface-enhanced raman spectroscopy through optical manipulation. Nano Lett. **6**, 2639–2641 (2006)
26. Jin, R.C., Cao, Y.W., Mirkin, C.A., Kelly, K.L., Schatz, G.C., Zheng, J.G.: Photoinduced conversion of silver nanospheres to nanoprisms. Science **294**, 1901–1903 (2001)
27. Aizpurua, J., Hanarp, P., Sutherland, D.S., Kall, M., Bryant, G.W., de Abajo, F.J.G.: Optical properties of gold nanorings. Phys. Rev. Lett. **90**, 057401 (2003)
28. Hao, F., Nehl, C.L., Hafner, J.H., Nordlander, P.: Plasmon resonances of a gold nanostar. Nano Lett. **7**, 729–732 (2007)
29. Raether, H.H.: Surface Plasmons. Springer (1988)
30. Lee, K.G., Kihm, H.W., Kihm, J.E., Choi, W.J., Kim, H., Ropers, C., Park, D.J., Yoon, Y. C., Choi, S.B., Woo, H., Kim, J., Lee, B., Park, Q.H., Lienau, C., Kim, D.S.: Vector field microscopic imaging of light. Nat. Photonics **1**, 53–56 (2007)
31. Schuck, P.J., Fromm, D.P., Sundaramurthy, A., Kino, G.S., Moerner, W.E.: Improving the mismatch between light and nanoscale objects with gold bowtie nanoantennas. Phys. Rev. Lett. **94**, 017402 (2005)
32. Taminiau, T.H., Moerland, R.J., Segerink, F.B., Kuipers, L., van Hulst, N.F.: lambda/4 Resonance of an optical monopole antenna probed by single molecule fluorescence. Nano Lett. **7**, 28–33 (2007)
33. Wang, W., Li, Z.P., Gu, B.H., Zhang, Z.Y., Xu, H.X.: Ag@SiO2 core-shell nanoparticles for probing spatial distribution of electromagnetic field enhancement via surface-enhanced raman scattering. ACS Nano **3**, 3493–3496 (2009)
34. Li, Z.P., Käll, M., Xu, H.: Optical forces on interacting plasmonic nanoparticles in a focused Gaussian beam. Phys. Rev. B **77**, 085412 (2008)
35. Lal, S., Clare, S.E., Halas, N.J.: Nanoshell-enabled photothermal cancer therapy: impending clinical impact. Acc. Chem. Res. **41**, 1842–1851 (2008)
36. Loo, C., Lowery, A., Halas, N.J., West, J., Drezek, R.: Immunotargeted nanoshells for integrated cancer imaging and therapy. Nano Lett. **5**, 709–711 (2005)
37. Ozbay, E.: Plasmonics: merging photonics and electronics at nanoscale dimensions. Science **311**, 189–193 (2006)

38. Kirchain, R., Kimerling, L.: A roadmap for nanophotonics. Nat. Photonics **1**, 303–305 (2007)
39. García de Abajo, F.J., Cordon, J., Corso, M., Schiller, F., Ortega, J.E.: Lateral engineering of surface states - towards surface-state nanoelectronics. Nanoscale **2**, 717–721 (2010)
40. Shegai, T., Chen, S., Miljkovic, V.D., Zengin, G., Johansson, P., Kall, M.: A bimetallic nanoantenna for directional colour routing. Nat. Commun. **2**, 2749–2763 (2011)
41. Li, Z.P., Shegai, T., Haran, G., Xu, H.X.: Multiple-particle nanoantennas for enormous enhancement and polarization control of light emission. ACS Nano **3**, 637–642 (2009)
42. Le Ru, E.C., Meyer, M., Etchegoin, P.G.: Proof of single-mokeule sensitivity in surface enhanced Raman scattering (SERS) by means of a two-analyte technique. J. Phys. Chem. B **110**, 1944–1948 (2006)